Rapid Communications

Accurate absolute core-electron binding energies of molecules, solids, and surfaces from first-principles calculations

J. Matthias Kahk
Department of Materials, Imperial College London, South Kensington, London SW7 2AZ, United Kingdom

Johannes Lischner*
Department of Physics, Department of Materials, and the Thomas Young Centre for Theory and Simulation of Materials, Imperial College London, London SW7 2AZ, United Kingdom

(Received 15 April 2019; published 14 October 2019)

Core-electron x-ray photoelectron spectroscopy is a powerful technique for studying the electronic structure and chemical composition of molecules, solids, and surfaces, but the interpretation of measured spectra and the assignment of peaks to atoms in specific chemical environments is often challenging. Here, we address this problem and demonstrate that accurate absolute core-electron binding energies can be obtained from the total energy difference of the ground state and a state with an explicit core hole when exchange and correlation effects are described by the strongly constrained and appropriately normed metageneralized gradient approximation and relativistic effects are included self-consistently even for light elements. We carry out calculations for molecules, solids, and surface species and find excellent agreement with available experimental measurements. For example, we find a mean absolute error of only 0.16 eV for a reference set of 103 molecular core-electron binding energies.

DOI: 10.1103/PhysRevMaterials.3.100801

I. INTRODUCTION

Core-level x-ray photoelectron spectroscopy (XPS) measures the energies required to remove core electrons from atoms in a given sample. As these energies depend sensitively on the atom's chemical environment, XPS is a powerful method for chemical analysis. In particular, core-level XPS finds widespread use in the characterization of the surfaces of solids, and insights gained from XPS measurements play a crucial role in developing our understanding of various surface chemical processes, including heterogeneous catalysis [1–4], the formation of electrified interfaces [5–7], corrosion and degradation [8–11], and adhesion [12–14]. A key challenge in applying XPS to complex materials is that it is often difficult to assign peaks in the XPS spectrum to specific chemical environments. Overcoming this peak assignment problem is critical in order to maximize the chemical insight gained from experimental XPS measurements.

Theoretical calculations of core-electron binding energies of atoms in different chemical environments have the potential to guide the interpretation of XPS spectra and several approaches have been developed to achieve this goal. The most common approaches are the Δ-self-consistent-field (ΔSCF) method where the core-electron binding energy is calculated as the total energy difference between the ground state and the final state with a core hole [15], and the related Slater-Janak transition state method [16,17]. These techniques yield *relative* core-electron binding energies, or binding energy shifts, that are in good agreement with experimental measurements for free molecules [18–23]. While calculated binding energy shifts are often very useful for the interpretation of XPS spectra, their use requires the existence of well-defined core-level reference energies which is not always guaranteed. It is therefore highly desirable to also calculate *absolute* core-electron binding energies, but these are often found to differ by multiple electron volts from measured values. Some works have reported the prediction of accurate absolute core-electron binding energies [20,24–26], but this typically relies on the fortuitous cancellation of errors arising from incomplete basis sets, limitations in the treatment of exchange and correlation effects, and the neglect or empirical treatment of relativistic effects [18]. The reliance on error cancellations ultimately limits the generality and the accuracy of these methods.

A variant of the ΔSCF scheme that overcomes some of the limitations of earlier studies was recently proposed by Pueyo Bellafont *et al.* [27]. Using the Tao, Perdew, Staroverov, and Scuseria [28] meta-generalized-gradient approximation (meta-GGA) exchange-correlation functional and fully uncontracted Gaussian basis sets, absolute 1*s* core-electron binding energies of B, C, N, O, and F atoms in free molecules were obtained that agree with experimental gas-phase measurements to within a mean absolute error of 0.21 eV, provided that corrections due to relativistic effects (ranging from 0.06 eV for B 1*s* to 0.75 eV for F 1*s*) are added to the calculated values.

As most XPS experiments are carried out on solids and surfaces, methods to calculate core-electron binding energies in such systems must be developed and several new approaches have been proposed in recent years. For example, Ozaki *et al.* introduced a formalism based on periodic density-functional theory (DFT) calculations where the effect of the core hole is simulated by introducing a penalty functional and the spurious interaction between periodically repeated core holes is

*j.lischner@imperial.ac.uk

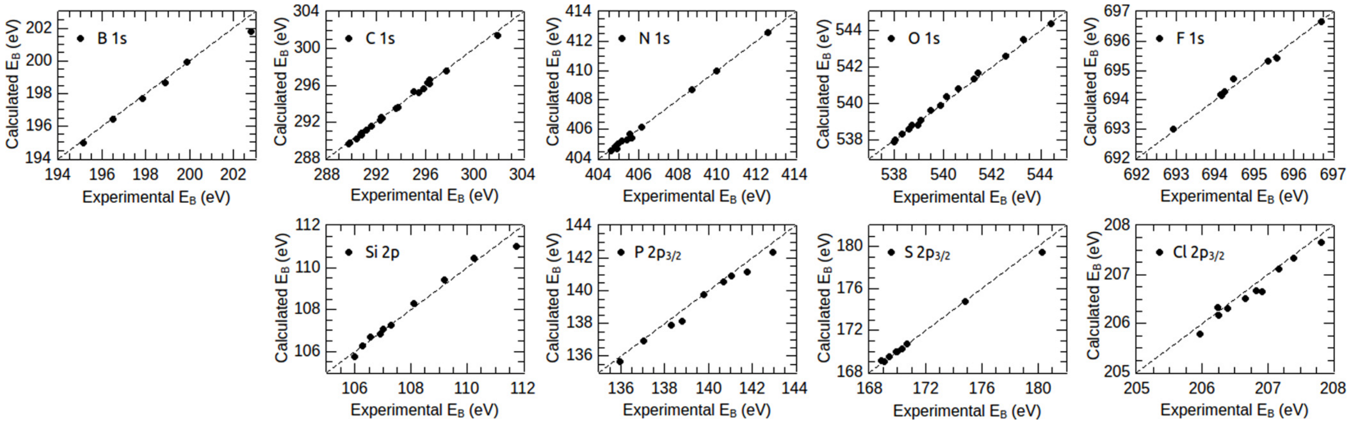

FIG. 1. A comparison of experimental and calculated core-electron binding energies for free molecules.

removed by the exact Coulomb cutoff method [29]. However, this method employs the frozen core approximation and thus neglects the screening effect from the relaxations of other core electrons resulting in significant quantitative inaccuracies. For example, for some simple molecules, such as NH_3 and N_2H_4, the calculated values differ by −0.9 and −1.28 eV from experimental data, respectively. Another method for calculating absolute core-electron binding energies in extended systems is based on the *GW* approach [30]. The high computational cost of *GW* calculations makes its application to chemically complex systems challenging, but preliminary tests have been published in [31] and [32]. Reference [31] reports relatively large deviations from experiment of several eV. The subsequent study, [32], addresses most of the limitations of [31] and reports that G_0W_0 calculations using a hybrid DFT starting point with a high fraction of exact exchange can predict absolute core-electron binding energies in a selection of free molecules with a mean error of 0.3 eV.

In this work, we propose a method based on the all-electron ΔSCF for calculating absolute core-electron binding energies of molecules, surfaces, and solids. In particular, we calculate total energies of the ground state and the final state which contains an explicit, spin-polarized core hole using DFT with the strongly constrained and appropriately normed (SCAN) exchange-correlation functional [33]. The SCAN functional is a nonempirical semilocal meta-GGA functional that obeys several exact constraints and combines generality, affordability, and good performance in benchmark calculations [33–38]. Relativistic effects are included self-consistently via the scaled zeroth-order regular approximation (ZORA) [39]. For orbital eigenvalues in Hartree-Fock calculations of free atoms, the scaled ZORA method yields accurate results (error relative to Dirac-Fock calculations less than 0.1 eV) for valence and shallow core levels of all elements and for all core and valence levels of light elements [39–42]. Extended systems are described using finite cluster models containing several hundred atoms, thereby allowing the ΔSCF method to be directly applied to solids and surface species.

II. RESULTS AND DISCUSSION

To assess the accuracy of our approach for free molecules, we carry out calculations for 75 molecules with a total of 103 core-electron binding energies (see Supplemental Material [43] for a full list of all molecules). This dataset contains 1*s* binding energies for the elements B, C, N, O, and F, and 2*p* binding energies for the elements Si, P, S, and Cl. To minimize the experimental error, we only included molecules whose core-electron binding energies were measured at least twice with the reported binding energies differing by no more than 0.3 eV. Subject to these criteria, the arithmetic averages of all reported experimental binding energies were then chosen as the reference values. In addition, the “weighted average” binding energies from Cavigliasso and Chong have also been included in the reference set [26]. The molecular structures were relaxed before the ΔSCF calculations of the core-electron binding energies. Figure 1 shows the calculated core-electron binding energies for free molecules and compares them to experimental gas-phase measurements (see also Table I). Our approach yields excellent agreement with experimental measurements with a mean error of only −0.09 eV and a mean absolute error of 0.16 eV. For 95 out of the 103 core-level binding energies of the dataset, the agreement with experiment is better than 0.3 eV. Given that core-electron binding energies for different chemical environments range over several eV for each of the considered 1*s* and 2*p* core levels, an accuracy better than 0.3 eV for the vast majority of cases means that the calculated binding energies are a

TABLE I. Summary of the calculated core-electron binding energies for free molecules and comparison to experiment. ME = mean error (theory − experiment). MAE = mean absolute error.

	B 1*s*	C 1*s*	N 1*s*	O 1*s*	F 1*s*	Si 2*p*	P $2p_{3/2}$	S $2p_{3/2}$	Cl $2p_{3/2}$	Total
Datapoints	6	22	13	16	8	10	9	9	10	103
ME (eV)	−0.29	−0.12	−0.02	0.00	0.02	−0.03	−0.33	−0.05	−0.14	−0.09
MAE (eV)	0.37	0.16	0.08	0.11	0.09	0.19	0.33	0.18	0.15	0.16

reliable guide for the interpretation of experimental spectra. For example, with very few exceptions, the energy ordering of almost all of the experimental datapoints is predicted correctly. To compare the performance of our approach to the method of Ref. [29], we have carried out calculations for the molecular dataset of Ref. [29]. We find that our approach yields a significantly smaller mean absolute error (0.19 vs 0.52 eV) and also a significantly smaller maximum error (0.70 vs 1.28 eV). We also carried out tests to probe the magnitudes of relativistic effects on calculated core-electron binding energies, and found that the differences between relativistic and nonrelativistic values are in very good agreement with the free atom relativistic corrections (obtained from atomic Dirac-Fock and Hartree-Fock calculations) used in Ref. [27], and about twice as large as the relativistic corrections predicted by the phenomenological model used in some earlier works, e.g., [24].

In the free molecule calculations, the eight core levels that differ most from the measured values are the B 1s core level in BF_3 (theoretical binding energy − experimental binding energy = −1.04 eV), S $2p_{3/2}$ in SF_6 (−0.84 eV), Si 2p in SiF_4 (−0.75 eV), P $2p_{3/2}$ in $P(CF_3)_3$ (−0.68 eV), P $2p_{3/2}$ in PF_3 (−0.63 eV), P $2p_{3/2}$ in POF_3 (−0.61 eV), C 1s in CF_4 (−0.45 eV), and P $2p_{3/2}$ in $P(OCH_3)_3$ (−0.37 eV). The relevant atoms in these molecules are in high oxidation states and we speculate that the observed errors are a consequence of the well-known difficulties of (semi-)local exchange-correlation functionals in describing systems with large charge transfer [44,45].

To calculate absolute core-electron binding energies of extended systems, we follow a two-step procedure that we have used to predict binding energy shifts in a previous study [46]. First, the atomic positions are relaxed using a periodic model of the (two-dimensional or three-dimensional) material. Next, a cluster is cut from the periodic structure and the ΔSCF method is used to calculate core-electron binding energies. In contrast to gas-phase experiments where the measured binding energies are referenced to the vacuum level (corresponding to a final state with one electron removed from the sample and promoted to the vacuum level), the binding energies obtained in XPS measurements on solids and surfaces are referenced to the Fermi level of the material. The corresponding core-electron binding energies can be obtained directly from a ΔSCF calculation where the core electron is promoted to an occupied state at the Fermi level (instead of being removed from the sample). In other words, the core-electron binding energy is calculated as the total energy difference between the ground state and a neutral final state with a core hole and an extra electron in the conduction band. This approach is valid as long as there are empty electronic states at the Fermi level, which is true for the metallic systems considered in this work. For systems with a band gap, the valence band maximum is a better reference point than the Fermi level. In that case, the core-electron binding energy can be calculated as the difference between the absolute core-electron binding energy referenced to the vacuum level, and the energy required to remove an electron from the valence band maximum which can be obtained from a separate ΔSCF calculation.

We have used the approach outlined above to calculate absolute core-electron binding energies in two elemental metals: Mg and Be. Specifically, we first carried out periodic DFT calculations using the SCAN functional to determine the equilibrium bulk lattice constants of Be and Mg (see Supplemental Material). Next, finite clusters containing 167 atoms were constructed from the bulk structure (see Fig. 2) and the 1s core-electron binding energies were calculated using the ΔSCF approach with the core hole being localized at an atom in the center of the cluster. Our results are summarized in Table II. For both Be and Mg, the calculated core-electron binding energies are within 0.3 eV of experimental values [47–55].

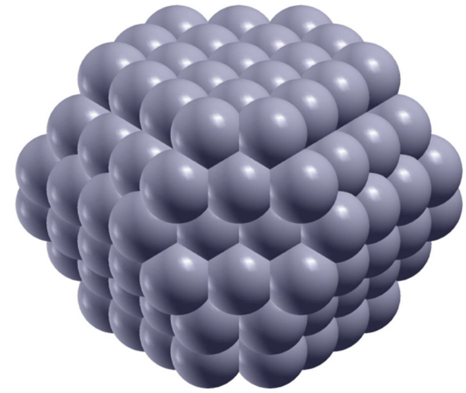

FIG. 2. The cluster of 167 atoms used to calculate the 1s core-electron binding energy in Be and Mg. The core hole is localized on an atom at the center of the cluster.

Finally we turn our attention to the prediction of core-electron binding energies of adsorbed molecules. We have carried out calculations for four molecules, H_2O, OH, CO, and HCOO, on Cu(111). In these calculations, a Cu cluster containing 163 Cu atoms, shown in Fig. 3, was used to model the Cu(111) surface. The relaxed geometries of the adsorbates on the surface were taken from our previous study [46]. For CO on Cu(111), the "top" adsorption site was used (where the CO sits directly above one of the Cu atoms). For water, an adsorbed H_2O molecule hydrogen bonded to two other adsorbed water molecules was considered. Table III compares the calculated absolute core-electron binding energies for the molecules adsorbed to the Cu(111) surface with experimental measurements. For these adsorbed molecules, "reference quality" experimental data is in general not available, making it difficult to judge the accuracy of the calculated values in a quantitative manner. However, in so far as can be determined, the agreement between theory and experiment is good. The calculated O 1s binding energies in adsorbed H_2O, OH, and HCOO are all within 0.35 eV of the experimental values; the

TABLE II. Calculated and experimental 1s binding energies (E_B) in metallic beryllium and magnesium.

	Be	Mg
Theoretical E_B (eV)	111.57	1303.07
Experimental E_B (eV)	111.82	1303.2

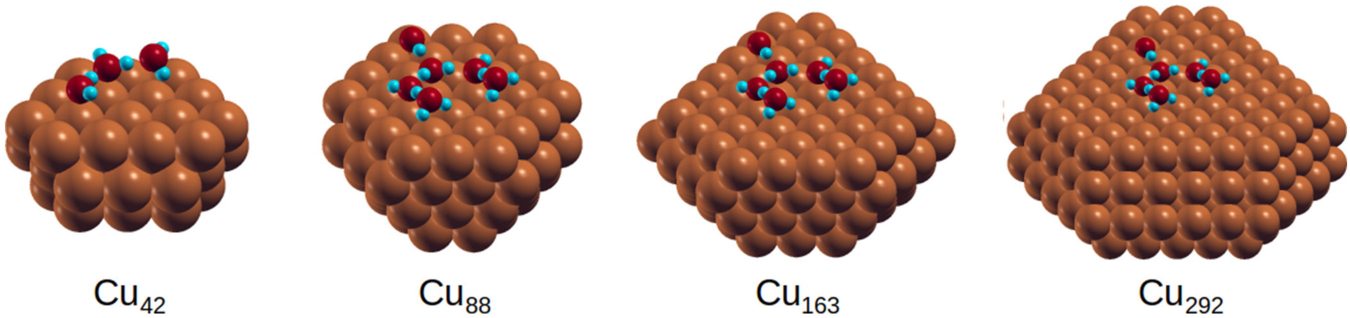

FIG. 3. The four Cu clusters that were used in ΔSCF calculations of the O 1s core-electron binding energy of adsorbed H_2O.

calculated C 1s binding energies of adsorbed CO and adsorbed HCOO are within 0.5 eV of the closest experimental data points, and the calculated O 1s binding energy in adsorbed CO lies in between two experimental values that differ from each other by almost 2 eV.

To establish that the obtained results are converged with respect to cluster size, we have calculated the O 1s binding energy of adsorbed H_2O on four different Cu clusters consisting of 42, 88, 163, and 292 Cu atoms, respectively. These clusters are shown in Fig. 3. Table IV shows that the calculated core-electron binding energies for the different cluster sizes vary by less than 0.15 eV.

III. CONCLUSIONS

We find that the ΔSCF approach yields accurate *absolute* core-electron binding energies for molecules, solids, and surfaces when the SCAN exchange-correlation energy functional is employed in conjunction with the scaled ZORA treatment of relativistic effects. Specifically, we find that our calculated binding energies agree with experiments to within 0.3 eV. This accuracy is usually sufficient to guide the interpretation of experimental XPS spectra and overcome the peak assignment problem that often limits the amount of information that can be extracted from XPS studies of complex materials. A shortcoming of the present approach is the perturbative treatment of spin-orbit coupling which is applied after the self-consistent field calculation. This reduces the accuracy of the approach for heavier elements. Future work will include a fully self-consistent treatment of spin-orbit coupling that will allow the accurate description of all elements in the periodic table.

TABLE III. A comparison of experimental and calculated core-electron binding energies for adsorbates on Cu(111).

Core level	Theor. E_B (eV)	Expt. E_B (eV)	
H_2O O 1s	532.95	533.0	[56]
		532.4	[57]
OH O 1s	531.15	531.50	[58]
CO C 1s	285.70	286.1	[59]
		286.2	[58]
CO O 1s	532.52	531.5	[59]
		533.4	[58]
		287.3	[57]
HCOO C 1s	286.82	288.2	[60]
		289.75	[61]
HCOO O 1s	531.25	531.5	[60]

ACKNOWLEDGMENTS

J.M.K. and J.L. acknowledge support from EPSRC under Grant No. EP/R002010/1. Via support by membership of the UK's HEC Materials Chemistry Consortium, which is funded by EPSRC (EP/L000202), this work used the ARCHER UK National Supercomputing Service [62].

APPENDIX: METHODS

All of the calculations reported in this work were carried out using the FHI-AIMS electronic structure code in which the Kohn-Sham wave functions are constructed as linear combinations of numerical atom-centered orbitals [63–65]. The computationally most demanding cluster calculations were performed on 16 supercomputer nodes with two 12-core Intel Xeon E5-2697 v2 processors per node, and took approximately 10 h to complete. The geometries of the free molecules and bulk Be and Mg were relaxed until the forces on all atoms were less than 5.0×10^{-3} eV/Å. Variable-cell optimization was used for Be and Mg. The FHI-AIMS default "tight" basis sets were used in the geometry optimizations [63]. For metallic Be and Mg, the Brillouin zone was sampled using a $12 \times 12 \times 8$ grid. For the adsorbates on Cu(111), relaxed geometries from our previous study were used [46]. In the ΔSCF calculations, special basis sets were used for the atoms where a core hole was created. These basis sets were constructed by adding additional, tighter core wave functions to the default basis sets of FHI-AIMS in order to permit the

TABLE IV. Dependence of the calculated absolute core-electron binding energy of an adsorbed water molecule on the size of the Cu cluster that is used to simulate the Cu(111) surface.

Species	Calculated O 1s E_B (eV)
H_2O on Cu_{42}	532.97
H_2O on Cu_{88}	532.85
H_2O on Cu_{163}	532.95
H_2O on Cu_{292}	532.84

relaxation of other core electrons in the presence of a core hole. Tests on simple molecules showed that the calculated core-electron binding energies obtained using the numerical basis sets were within 0.08 eV of the values obtained for the same systems using large, uncontracted Gaussian basis sets derived from the pcJ-3 basis sets of Jensen [66]. Full details of the basis sets used in this work are given in the Supplemental Material. When calculating the total energy of the final state, the core hole was introduced by constraining the occupancy of a specific Kohn-Sham state in one of the spin channels. In cases where the molecule contains a number of atoms of the same element, the localization of the core hole at a specific atom was ensured by introducing a fictitious extra charge of $0.1e$ during the first step of the self-consistent field cycle at the desired site which attracts the core hole. The fictitious charge was removed immediately afterwards and the constrained self-consistent field calculations were run in the usual manner.

All of the reported calculations were scalar relativistic. Therefore, the calculated $2p$ core-electron binding energies correspond to the weighted average of the $2p_{1/2}$ and $2p_{3/2}$ states. For comparisons to experimental data, the as-obtained $2p$ binding energies were used for Si. For P, S, and Cl, the position of the $2p_{3/2}$ peak is usually reported experimentally. The theoretical $2p_{3/2}$ binding energies reported in this work were obtained by subtracting 1/3 of the experimental spin-orbit splitting (0.29 eV for P $2p$, 0.387 eV for S $2p$, and 0.533 eV for Cl $2p$) from the ΔSCF value. Very similar binding energies (to within less than 0.05 eV) are obtained if theoretical spin-orbit splittings, as determined from the eigenvalue difference after the perturbative SOC calculations [67], are used instead.

[1] K. Murugappan, E. M. Anderson, D. Teschner, T. E. Jones, K. Skorupska, and Y. Román-Leshkov, Operando NAP-XPS unveils differences in MoO_3 and Mo_2C during hydrodeoxygenation, Nat. Catal. **1**, 960 (2018).

[2] K. A. Goulas, A. V. Mironenko, G. R. Jenness, T. Mazal, and D. G. Vlachos, Fundamentals of C-O bond activation on metal oxide catalysts, Nat. Catal. **2**, 269 (2019).

[3] S. Kattel, P. J. Ramírez, J. G. Chen, J. A. Rodriguez, and P. Liu, Active sites for CO_2 hydrogenation to methanol on Cu/ZnO catalysts, Science **355**, 1296 (2017).

[4] N. Feng, Q. Wang, A. Zheng, Z. Zhang, J. Fan, S.-B. Liu, J.-P. Amoureux, and F. Deng, Understanding the high photocatalytic activity of (B, Ag)-codoped TiO_2 under solar-light irradiation with XPS, solid-state NMR, and DFT calculations, J. Am. Chem. Soc. **135**, 1607 (2013).

[5] M. Favaro, B. Jeong, P. N. Ross, J. Yano, Z. Hussain, Z. Liu, and E. J. Crumlin, Unravelling the electrochemical double layer by direct probing of the solid/liquid interface, Nat. Commun. **7**, 12695 (2016).

[6] S. G. Booth, A. M. Tripathi, I. Strashnov, R. A. W. Dryfe, and A. S. Walton, The offset droplet: A new methodology for studying the solid/water interface using x-ray photoelectron spectroscopy, J. Phys.: Condens. Matter **29**, 454001 (2017).

[7] S. Axnanda, E. J. Crumlin, B. Mao, S. Rani, R. Chang, P. G. Karlsson, M. O. M. Edwards, M. Lundqvist, R. Moberg, P. Ross, Z. Hussain, and Z. Liu, Using "tender" x-ray ambient pressure x-ray photoelectron spectroscopy as a direct probe of solid-liquid interface, Sci. Rep. **5**, 9788 (2015).

[8] M. Bouanis, M. Tourabi, A. Nyassi, A. Zarrouk, C. Jama, and F. Bentiss, Corrosion inhibition performance of 2,5-bis(4-dimethylaminophenyl)-1,3,4-oxadiazole for carbon steel in HCl solution: Gravimetric, electrochemical and XPS studies, Appl. Surf. Sci. **389**, 952 (2016).

[9] H. Zarrok, A. Zarrouk, B. Hammouti, R. Salghi, C. Jama, and F. Bentiss, Corrosion control of carbon steel in phosphoric acid by purpald—Weight loss, electrochemical and XPS studies, Corros. Sci. **64**, 243 (2012).

[10] G. S. Parkinson, Iron oxide surfaces, Surf. Sci. Rep. **71**, 272 (2016).

[11] F. Orlando, A. Waldner, T. Bartels-Rausch, M. Birrer, S. Kato, M.-T. Lee, C. Proff, T. Huthwelker, A. Kleibert, J. van Bokhoven, and M. Ammann, The environmental photochemistry of oxide surfaces and the nature of frozen salt solutions: A new *in situ* XPS approach, Top. Catal. **59**, 591 (2016).

[12] Y. Yoshida, K. Nagakane, R. Fukuda, Y. Nakayama, M. Okazaki, H. Shintani, S. Inoue, Y. Tagawa, K. Suzuki, J. De Munck, and B. Van Meerbeek, Comparative study on adhesive performance of functional monomers, J. Dent. Res. **83**, 454 (2004).

[13] M. Noeske, J. Degenhardt, S. Strudthoff, and U. Lommatzsch, Plasma jet treatment of five polymers at atmospheric pressure: Surface modifications and the relevance for adhesion, Int. J. Adhes. Adhes. **24**, 171 (2004).

[14] Y. Wang, J. Xue, Q. Wang, Q. Chen, and J. Ding, Verification of icephobic/anti-icing properties of a superhydrophobic surface, ACS Appl. Mater. Interfaces **5**, 3370 (2013).

[15] P. S. Bagus, Self-Consistent-Field Wave Functions for Hole States of Some Ne-Like and Ar-Like Ions, Phys. Rev. **139**, A619 (1965).

[16] J. C. Slater, Statistical exchange-c in the self-consistent field, *Advances in Quantum Chemistry* (Elsevier, New York, 1972), Vol. 6, pp. 1–92.

[17] A. R. Williams, R. A. deGroot, and C. B. Sommers, Generalization of Slater's transition state concept, J. Chem. Phys. **63**, 628 (1975).

[18] F. Viñes, C. Sousa, and F. Illas, On the prediction of core level binding energies in molecules, surfaces and solids, Phys. Chem. Chem. Phys. **20**, 8403 (2018).

[19] Y. Takahata and A. Dos Santos Marques, Accurate core-electron binding energy shifts from density functional theory, J. Electron Spectrosc. Relat. Phenom. **178-179**, 80 (2010).

[20] I. Tolbatov and D. M. Chipman, Comparative study of Gaussian basis sets for calculation of core electron binding energies in first-row hydrides and glycine, Theor. Chem. Acc. **133**, 1560 (2014).

[21] Y. Takahata and D. P. Chong, Estimation of Hammett sigma constants of substituted benzenes through accurate density-functional calculation of core-electron binding energy shifts, Int. J. Quantum Chem. **103**, 509 (2005).

[22] N. Pueyo Bellafont, G. Álvarez Saiz, F. Viñes, and F. Illas, Performance of Minnesota functionals on predicting core-level binding energies of molecules containing main-group elements, Theor. Chem. Acc. **135**, 35 (2016).

[23] N. Pueyo Bellafont, F. Viñes, W. Hieringer, and F. Illas, Predicting core level binding energies shifts: Suitability of the projector augmented wave approach as implemented in VASP, J. Comput. Chem. **38**, 518 (2017).

[24] Y. Takahata, A. D. S. Marques, and R. Custodio, Accurate calculation of C1s core electron binding energies of some carbon hydrates and substituted benzenes, J. Mol. Struct.: THEOCHEM **959**, 106 (2010).

[25] M. S. Oakley and M. Klobukowski, ΔDFT/MIX: A reliable and efficient method for calculating core electron binding energies of large molecules, J. Electron Spectrosc. Relat. Phenom. **227**, 44 (2018).

[26] G. Cavigliasso and D. P. Chong, Accurate density-functional calculation of core-electron binding energies by a total-energy difference approach, J. Chem. Phys. **111**, 9485 (1999).

[27] N. Pueyo Bellafont, F. Viñes, and F. Illas, Performance of the TPSS functional on predicting core level binding energies of main group elements containing molecules: A good choice for molecules adsorbed on metal surfaces, J. Chem. Theory Comput. **12**, 324 (2016).

[28] J. Tao, J. P. Perdew, V. N. Staroverov, and G. E. Scuseria, Phys. Rev. Lett. **91**, 146401 (2003).

[29] T. Ozaki and C.-C. Lee, Absolute Binding Energies of Core Levels in Solids from First Principles, Phys. Rev. Lett. **118**, 026401 (2017).

[30] T. Aoki and K. Ohno, Accurate quasiparticle calculation of x-ray photoelectron spectra of solids, J. Phys.: Condens. Matter **30**, 21LT01 (2018).

[31] M. J. van Setten, R. Costa, F. Viñes, and F. Illas, Assessing *GW* approaches for predicting core level binding energies, J. Chem. Theory Comput. **14**, 877 (2018).

[32] D. Golze, J. Wilhelm, M. J. van Setten, and P. Rinke, Core-level binding energies from *GW*: An efficient full-frequency approach within a localized basis, J. Chem. Theory Comput. **14**, 4856 (2018).

[33] J. Sun, A. Ruzsinszky, and J. P. Perdew, Strongly Constrained and Appropriately Normed Semilocal Density Functional, Phys. Rev. Lett. **115**, 036402 (2015).

[34] J. Sun, R. C. Remsing, Y. Zhang, Z. Sun, A. Ruzsinszky, H. Peng, Z. Yang, A. Paul, U. Waghmare, X. Wu, M. L. Klein, and J. P. Perdew, Accurate first-principles structures and energies of diversely bonded systems from an efficient density functional, Nat. Chem. **8**, 831 (2016).

[35] E. B. Isaacs and C. Wolverton, Performance of the strongly constrained and appropriately normed density functional for solid-state materials, Phys. Rev. Mater. **2**, 063801 (2018).

[36] M. Marianski, A. Supady, T. Ingram, M. Schneider, and C. Baldauf, Assessing the accuracy of across-the-scale methods for predicting carbohydrate conformational energies for the examples of glucose and α-maltose, J. Chem. Theory Comput. **12**, 6157 (2016).

[37] L. Goerigk, A. Hansen, C. Bauer, S. Ehrlich, A. Najibi, and S. Grimme, A look at the density functional theory zoo with the advanced GMTKN55 database for general main group thermochemistry, kinetics and noncovalent interactions, Phys. Chem. Chem. Phys. **19**, 32184 (2017).

[38] D. J. Tozer and M. J. G. Peach, Molecular excited states from the SCAN functional, Mol. Phys. **116**, 1504 (2018).

[39] E. van Lenthe, E. J. Baerends, and J. G. Snijders, Relativistic total energy using regular approximations, J. Chem. Phys. **101**, 9783 (1994).

[40] S. Faas, J. Snijders, J. van Lenthe, E. van Lenthe, and E. Baerends, The ZORA formalism applied to the Dirac-Fock equation, Chem. Phys. Lett. **246**, 632 (1995).

[41] K. G. Dyall and E. van Lenthe, Relativistic regular approximations revisited: An infinite-order relativistic approximation, J. Chem. Phys. **111**, 1366 (1999).

[42] W. Klopper, J. H. van Lenthe, and A. C. Hennum, An improved *ab initio* relativistic zeroth-order regular approximation correct to order $1/c^2$, J. Chem. Phys. **113**, 9957 (2000).

[43] See Supplemental Material at http://link.aps.org/supplemental/10.1103/PhysRevMaterials.3.100801 for the full details of the experimental dataset of 103 core electron binding energies from gas phase photoemission measurements, and the results of the respective theoretical calculations; the basis sets used throughout this work, the geometries of the clusters used for calculating core electron binding energies of adsorbates and solids, and the relaxed lattice parameters of bulk Be and Mg obtained using the SCAN functional.

[44] J. P. Perdew, R. G. Parr, M. Levy, and J. L. Balduz, Density-Functional Theory for Fractional Particle Number: Derivative Discontinuities of the Energy, Phys. Rev. Lett. **49**, 1691 (1982).

[45] A. J. Cohen, P. Mori-Sanchez, and W. Yang, Insights into current limitations of density functional theory, Science **321**, 792 (2008).

[46] J. M. Kahk and J. Lischner, Core electron binding energies of adsorbates on Cu(111) from first-principles calculations, Phys. Chem. Chem. Phys. **20**, 30403 (2018).

[47] C. Powell, Recommended Auger parameters for 42 elemental solids, J. Electron Spectrosc. Relat. Phenom. **185**, 1 (2012).

[48] C. Powell, Elemental binding energies for x-ray photoelectron spectroscopy, Appl. Surf. Sci. **89**, 141 (1995).

[49] L. Ley, F. R. McFeely, S. P. Kowalczyk, J. G. Jenkin, and D. A. Shirley, Many-body effects in x-ray photoemission from magnesium, Phys. Rev. B **11**, 600 (1975).

[50] J. Fuggle, XPS, UPS and XAES studies of oxygen adsorption on polycrystalline Mg at ∼100 and ∼300 K, Surf. Sci. **69**, 581 (1977).

[51] D. R. Jennison, P. Weightman, P. Hannah, and M. Davies, Calculation of Mg atom-metals XPS and Auger shifts using a ΔSCF excited atom model, J. Phys. C **17**, 3701 (1984).

[52] T. D. Thomas and P. Weightman, Valence electronic structure of AuZn and AuMg alloys derived from a new way of analyzing Auger-parameter shifts, Phys. Rev. B **33**, 5406 (1986).

[53] X. Peng, D. Edwards, and M. Barteau, Reactions of O_2 and H_2O with magnesium nitride films, Surf. Sci. **195**, 103 (1988).

[54] K. Yoshimura, Y. Yamada, S. Bao, K. Tajima, and M. Okada, Degradation of switchable mirror based on Mg-Ni alloy thin film, Jpn. J. Appl. Phys. **46**, 4260 (2007).

[55] A. Fischer, H. Köstler, and L. Schlapbach, Hydrogen in magnesium alloys and magnesium interfaces: Preparation, electronic properties and interdiffusion, J. Less-Common Met. **172**, 808 (1991).

[56] M. W. Roberts, Low energy pathways and precursor states in the catalytic oxidation of water and carbon dioxide at metal surfaces and comparisons with ammonia oxidation, Catal. Lett. **144**, 767 (2014).

[57] M. Favaro, H. Xiao, T. Cheng, W. A. Goddard III, J. Yano, and E. J. Crumlin, Subsurface oxide plays a critical role in CO_2 activation by Cu(111) surfaces to form chemisorbed CO_2, the first step in reduction of CO_2, Proc. Natl. Acad. Sci. USA **114**, 6706 (2017).

[58] K. Mudiyanselage, S. D. Senanayake, L. Feria, S. Kundu, A. E. Baber, J. Graciani, A. B. Vidal, S. Agnoli, J. Evans, R. Chang, S. Axnanda, Z. Liu, J. F. Sanz, P. Liu, J. A. Rodriguez, and D. J. Stacchiola, Importance of the metal-oxide interface in catalysis: *In situ* studies of the water-gas shift reaction by ambient-pressure x-ray photoelectron spectroscopy, Angew. Chem., Int. Ed. **52**, 5101 (2013).

[59] B. Eren, C. Heine, H. Bluhm, G. A. Somorjai, and M. Salmeron, Catalyst chemical state during CO oxidation reaction on Cu(111) studied with ambient-pressure x-ray photoelectron spectroscopy and near edge x-ray adsorption fine structure spectroscopy, J. Am. Chem. Soc. **137**, 11186 (2015).

[60] J. Nakamura, Y. Kushida, Y. Choi, T. Uchijima, and T. Fujitani, X-ray photoelectron spectroscopy and scanning tunnel microscope studies of formate species synthesized on Cu(111) surfaces, J. Vac. Sci. Technol., A **15**, 1568 (1997).

[61] Y. Yang, J. Evans, J. A. Rodriguez, M. G. White, and P. Liu, Fundamental studies of methanol synthesis from CO_2 hydrogenation on Cu(111), Cu clusters, and Cu/ZnO(0001), Phys. Chem. Chem. Phys. **12**, 9909 (2010).

[62] https://www.archer.ac.uk/documentation/user-guide/introduction.php.

[63] V. Blum, R. Gehrke, F. Hanke, P. Havu, V. Havu, X. Ren, K. Reuter, and M. Scheffler, *Ab initio* molecular simulations with numeric atom-centered orbitals, Comput. Phys. Commun. **180**, 2175 (2009).

[64] V. Havu, V. Blum, P. Havu, and M. Scheffler, Efficient integration for all-electron electronic structure calculation using numeric basis functions, J. Comput. Phys. **228**, 8367 (2009).

[65] R. Strange, F. Manby, and P. Knowles, Automatic code generation in density functional theory, Comput. Phys. Commun. **136**, 310 (2001).

[66] F. Jensen, The optimum contraction of basis sets for calculating spin-spin coupling constants, Theor. Chem. Acc. **126**, 371 (2010).

[67] W. P. Huhn and V. Blum, One-hundred-three compound band-structure benchmark of post-self-consistent spin-orbit coupling treatments in density functional theory, Phys. Rev. Mater. **1**, 033803 (2017).